International Communications in Heat and Mass Transfer 39 (2012) 439–448

Contents lists available at SciVerse ScienceDirect

International Communications in Heat and Mass Transfer

journal homepage: www.elsevier.com/locate/ichmt

Investigation of basic molecular gas structural effects on hydrodynamics and thermal behaviors of rarefied shear driven micro/nano flow using DSMC☆

Omid Ejtehadi, Ehsan Roohi *, Javad Abolfazli Esfahani

Department of Mechanical Engineering, Faculty of Engineering, Ferdowsi University of Mashhad, Mashhad, Iran, P.O. Box: 91775-1111

ARTICLE INFO

Available online 30 January 2012

Keywords:
DSMC
Couette flow
Molecular structures
Heat flux
Shear stress

ABSTRACT

In the present work, rarefied gas flow between two parallel moving plates maintained at the same uniform temperature is simulated using the direct simulation Monte Carlo (DSMC) method. Heat transfer and shear stress behavior in the micro/nano-Couette flow is studied and the effects of the important molecular structural parameters such as molecular diameter, mass, degrees of freedom and viscosity–temperature index on the macroscopic behavior of gases are investigated. Velocity, temperature, heat flux and shear stress in the domain are studied in details. Finally, a discussion on the role of the molecular structural parameters in the decrease or increase of amounts of hydrodynamics and thermal properties of the gas is presented.

1. Introduction

In recent years, prediction of rarefied gas flow and heat transfer behavior of micro/nano flows attracted attention of researchers due to the wide applications of micro/nanoelectromechanical system (MEMS/NEMS) devices such as micro-valve, micro-turbine, micro-pump and micro/nano-nozzles. To measure the degree of rarefaction the Knudsen number (Kn) is defined as the ratio of mean free path of the gas molecules to the characteristic length of the geometry ($Kn = \lambda/L$). When the Knudsen number is sufficiently large, the gas rarefaction is the main parameter to evaluate these systems [1]. Flow regimes are also classified on the basis of the Knudsen number into: continuum ($Kn \leq 0.01$), slip flow ($0.01 < Kn < 0.1$), transition flow ($0.1 < Kn < 10$) and free molecular ($Kn \geq 10$).

When there is a continuum breakdown, the conventional method to describe gas flows, i.e., the Navier–Stokes (NS) equations fails to predict the flow and the solutions are to be established based on the kinetic principles such as those in treating the Boltzmann equation. Direct simulation Monte Carlo (DSMC) is shown to be the most accurate numerical tool to handle the complexity of the Boltzmann equation [2]. DSMC method possesses many advantages such as simplicity of application, unconditional stability, and ease of modeling complex physical flow. However, the computational cost is larger than the traditional CFD approaches.

Shear-driven flows such as Couette flow are encountered in micro-motor, comb mechanism, and micro/nano-bearing. In this study we choose the well known problem of planar Couette flow, i.e., a gas confined between two infinite parallel plates which are at the same temperature but moving relative to each other. Micro/nano-Couette flow has been widely studied in the literature. For example, Morris et al. [3] investigated slip length in a dilute gas in Couette and Poiseuille flow using molecular dynamics (MD) and DSMC and found that slip length is accurately given by Maxwell theory in the entire Knudsen regime. Beskok et al. [4] reported a detailed analysis of the effects of compressibility and rarefaction on pressure-driven and shear-driven microflows. They found that compressibility and rarefaction are competing phenomena and both require consideration in microfluidic analysis. Marques et al. [5] investigated gaseous micro-Couette flow with the NS equations and compared their results with DSMC method in the continuum and transition regimes. Their comparison between the NS and DSMC solutions for the heat flux vector shows that slip and jump boundary conditions do not necessarily depend on the velocities of the plates. Xue et al. [6–8] analyzed the micro-Couette flow using DSMC method, the NS, and the Burnett equations. They found that the rarefaction has a significant effect on velocity, temperature and pressure, especially for high Knudsen number flows. They stated that the non-dimensional parameter Prandtl–Ekcert (*PrEc*) characterizing convective heat transfer in the Couette flow increases as flow rarefies more. Their prediction of shear stress and heat flux at wall shows the superiority of the Burnett equations than the NS in the micro-Couette solution. Meanwhile the Burnett equations with the slip boundary condition, which is proportional to the Knudsen number, cannot be extended to the transition flow regime. McNenly et al. [9] constructed models to capture the Knudsen number dependence of the slip and viscosity model coefficients by a linear least-squares fit of the NS solution to the non-equilibrium solution obtained using the DSMC method for the Couette and Poiseuille flows. Roy and Chakraborty [10] investigated near-wall effects in micro scale laminar Couette flow for Knudsen number varying from 10^{-3} to 10^{-1} and found that for values of the

☆ Communicated by W.J. Minkowycz.

* Corresponding author.
E-mail address: e.roohi@ferdowsi.um.ac.ir (E. Roohi).

0735-1933/$ – see front matter © 2012 Elsevier Ltd. All rights reserved.
doi:10.1016/j.icheatmasstransfer.2012.01.010

Knudsen number of the order of 10^{-2} or higher the heat transfer predictions from their model deviate significantly from the classical slip flow based predictions in which wall-adjacent layer effects are not considered. More recently, Frezzotti et al. [11] proposed a moment method based on the linearized Bhatnagar–Gross–Krook (BGK) kinetic model equation and applied the method to the cases of Couette, Poiseuille and cavity flow. Their results showed that excellent approximations of exact solutions of the kinetic model equation could be obtained using a small number of moment equations. Gu and Emerson [12] used high order moment approach, i.e., regularized 26 moment equations, for capturing non-equilibrium phenomena in the transition regime for the Couette flow. Their new set of equations overcomes many of the limitations observed in the regularized 13 moment equations and had good accuracy compared to the DSMC solution. Kumar et al. [13] investigated the accuracy of the solution of statistical Bhatnagar–Gross–Krook (BGK) and ellipsoidal statistical BGK (ESBGK) equations in comparison with the DSMC solution in Couette flow. They showed that these methods are numerically more efficient than the DSMC method for a flow simulation in conditions that are presently at the comfort-level limit for DSMC computations.

The objective of present work is to provide a deeper understanding of the effect of four important molecular structures, i.e., molecular diameter, mass, degrees of freedom and viscosity–temperature index on the micro/nano flow behavior. Although simulation of Couette flow has been implemented before, the specific contributions of this work in the study of micro/nano-Couette flow are investigation of the behavior of important engineering parameters, like heat flux and shear stress. In addition we investigate the governing physical behavior due to variation of molecular diameter, mass, degrees of freedom and viscosity–temperature index for the first time. The approximate analytical solutions for the planar Couette flows are available within the framework of continuum fluid mechanics subject to velocity slip and temperature jump boundary conditions and valid for the low-velocity (subsonic) and low Knudsen number ($Kn \leq 0.1$) flows [1,5]. Consequently, we compare our DSMC temperature, velocity, shear stress and heat flux distribution with the approximate analytical solution.

2. Problem statement

Planar Couette flow involves a gas trapped between two infinite plate at $y = \pm h/2$ moving relative to each other in opposite directions with a constant velocity $\pm U_w$ and maintained at the same constant temperature, T_w. The flow is driven by the shear stress of moving plates and depends on the y coordinate only. Therefore the flow is considered steady, one dimensional and compressible. The flow velocity generated by shear is assumed to have only an x component varying only in the y direction. Temperature profiles are parabolic and are generated by the viscous dissipation. The amount of heat flux in y direction is zero in the center of the channel and increases towards the plates. The shear stress in the domain is constant. Also the external forces are assumed to be absent.

2.1. The DSMC method

The Boltzmann equation describes the gas flow behavior in all the rarefaction regimes. The DSMC method is proved to be the most accurate numerical tool to solve the Boltzmann equation based on the direct statistical simulation of the molecular processes described by the kinetic theory [2]. The algorithm includes four primary steps: moving the particles, indexing them, collision simulation, and sampling the flow-field. The primary principle of DSMC is to decouple the motion and collision of particles during one time step. The implementation of DSMC needs breaking down the computational domain into a collection of grid cells. The cells are divided into subcells in each direction. The subcells are then utilized to facilitate the selection of collision pairs. After fulfilling all molecular movements, the collision between molecules is simulated in each cell separately in a statistical manner. The random selection of the particles from a cell for binary collisions requires that the cell size to be a small fraction of the gas mean free path. The decoupling between the particles movement and collisions is correct if the time step is a small fraction of the mean collision time. Number of particles per cell should be high enough, around 20, to avoid repeated binary collisions between the same particles. In the entire computational domain, an arbitrary initial state of gas particles is specified and the desired boundary conditions are imposed at time zero. Particles movement and binary collisions are performed separately. After achieving steady flow condition, sampling of molecular properties within each cell is fulfilled during sufficient time period to avoid statistical scattering. More details on DSMC algorithm are given in Ref. [2,14]. In the current study, variable hard sphere (VHS) collision model is used and the collision pair is chosen based on the no time counter (NTC) method. We use diffuse reflection model with the full thermal accommodation coefficient for the walls and set the time step and cell dimensions equal to 10^{-13} (s) and 10^{-8} (m), respectively. These values are set in such a way that they do not exceed mean collision time and mean free path, respectively.

3. Results and discussion

The DSMC code used by Roohi and coworkers [15–19] for simulation of different geometries like micronozzle, microchannel and backward facing step is applied and modified to simulate micro-Couette flow. Argon with molecular mass of $m = 6.63 \times 10^{-26}$ kg, viscosity–temperature index of $\omega = 0.81$, variable hard-sphere diameter of $d_{vhs} = 4.17 \times 10^{-10}$ m and specific heat ratio of $\gamma = 1.667$ is considered as the base gas. By varying the favorable parameter and keeping other molecular parameters constant, we simulate some imaginary gases to investigate the effects of four molecular parameters on the flow behavior. The properties of imaginary gases are a combination of properties of real gases and the variation of the investigated parameter is in the range of corresponding value in real gases. Simulated imaginary gases and their properties are shown in Table 1. Simulations are performed for $Kn = 0.1$ and $M_{wall} = 1.05$, here. The reason for using $Kn = 0.1$ is that most applications of MEMS devices are in the slip and early transition regimes. M_{wall} is the wall Mach number defined as the ratio of U_w to the parameter $\sqrt{kT_w/m}$ and is specified by varying the driving velocity of both plates U_w. In all cases, the simulated gas and the wall temperature are considered at a reference temperature of $T_{ref} = 273$ K.

The macroscopic properties of the interest in the present work are viscous shear and heat flux, derived using molecular gas dynamics [2].

Table 1
Simulated cases: imaginary gases ($Kn = 0.1$–$M_{wall} = 1.05$).

Gas	Diameter ($d \times 10^{-10}$ m)	Degrees of freedom (ζ)	Molecular mass ($m \times 10^{-27}$ kg)	Viscosity index (ω)
A	2			
B	3.5	3	66.3	0.81
C	5			
D	6.5			
E		3		
F	4.17	5	66.3	0.81
G		6.1		
H		6.7		
I			10	
J			20	
K	4.17	3	40	0.81
L			80	
M			160	
N				0.6
O	4.17	3	66.3	0.8
P				1

Viscous stress tensor $\boldsymbol{\tau}$, is defined as the negative of the pressure tensor with the static pressure subtracted from the normal components [2].

$$\tau = \tau_{ij} = -\left(\rho\overline{c'_i c'_j} - \delta_{ij} p\right) \tag{1}$$

where c_i and c_j are the components of c the velocity of molecule relative to stream velocity, i.e., thermal velocity and p is the pressure tensor defined as:

$$p = p_{ij} = \rho\overline{c'_i c'_j} \tag{2}$$

The heat flux vector is defined as:

$$q = \frac{1}{2}\rho\overline{c'^2 c'} + n\overline{\varepsilon_{int} c'} \tag{3}$$

where, ε_{int} is the internal energy of a single molecule.

In figures, the ordinate is normalized by the distance between the parallel plates h. Flow velocity and temperature are normalized by the relative velocity of the plates U_w and the temperature of the wall T_w, respectively.

Also heat flux and shear stress are normalized by the parameters, $\rho_\infty U_w C_p T_w$ and $\frac{1}{2}\rho_\infty U_w^2$, respectively. Here, ρ_∞ and C_p are the free stream density and the specific heat capacity of argon, respectively. The normalized heat flux and shear stress are referred to as the heat flux coefficient (C_h) and the friction coefficient (C_f), respectively, in the figures.

3.1. Grid study and validation

To achieve grid independent solutions, we simulate argon flow in a channel using three different grid resolutions in y direction. We kept number of particles per cell constant, i.e., average of 300 particles per cell, and set Knudsen and wall Mach number to 0.1 and 1.05 respectively. Although the problem is one-dimensional, we employed a two-dimensional code and imposed periodic boundary condition on both sides of the domain to correctly simulate infinite length plates. Fig. 1 shows the velocity, temperature, heat flux and shear stress profiles of argon gas for the three investigated grids, i.e., Grid 1 (150,000 particles in 10×50 cells), Grid 2 (300,000 particles in 10×100 cells) and Grid 3 (450,000 particles in 10×150 cells). It is observed that Grids 2 and 3 give almost identical velocity, temperature, heat flux and shear stress profiles. More dependency on the grid on the temperature and heat flux profiles than velocity and shear stress profiles is observed, but solutions of Grid 2 and 3 are quite close to each other. Therefore, we continue our study using Grid 2.

The approximate analytical NS solutions subject to velocity slip and temperature jump boundary conditions are available and valid for the planar Couette flow [4,5,10,20]. Marques et al. [5] derived

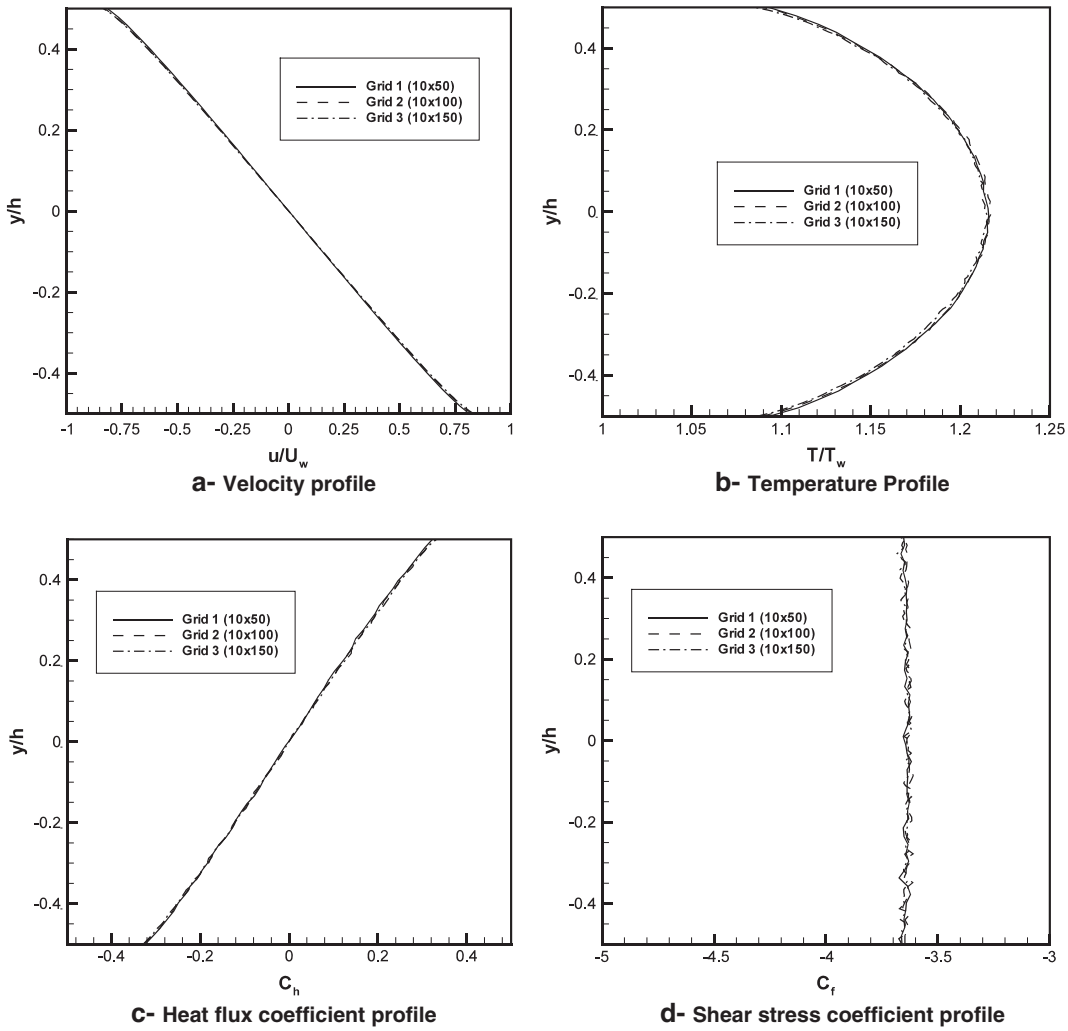

Fig. 1. Grid study test (Profiles).

the solution for the streamwise velocity and the temperature profile in the Couette flow as follows:

$$U = \frac{U_w}{1 + k_0 Kn}\frac{2y}{h} \tag{4}$$

$$T = T_w + \frac{2m}{15k}(1 + 2k_1 Kn)\left(\frac{U_w}{1 + k_0 Kn}\right)^2 - \frac{2m}{15k}\left(\frac{U_w}{1 + k_0 Kn}\right)^2\left(\frac{2y}{h}\right)^2 \tag{5}$$

where k and m are the Boltzmann constant and the mass of a gas molecule, respectively. For hard sphere gases, k_0 and k_1 are two constants with values 1.111 and 2.127, respectively [5]. The heat flux may be derived using the relationship below [5]:

$$q_y = \mu\left(\frac{U_w}{1 + k_0 Kn}\right)^2 \frac{4y}{h^2} \tag{6}$$

$\mu = (2mkT_0/\pi)^{1/2} n_0 \lambda$ is the viscosity coefficient with n_0 representing the number density. It can be deduced that shear stress is calculated by substituting viscosity coefficient and dU/dy derived from Eq. (4) into the familiar shear equation for Newtonian fluids ($\tau_{xy} = -\mu dU/dy$):

$$\tau_{xy} = \mu \frac{U_w}{1 + k_0 kn}\frac{2}{h} \tag{7}$$

Fig. 2 shows the comparison of velocity, temperature, heat flux and shear stress with the approximate analytical solution of Ref. [5] and DSMC solution of Ref. [12]. In this comparison the Knudsen number is equal to 0.1 and the wall Mach number is 0.21. The present case is a slip regime simulation and it is observed that there is a good agreement between our solution and the DSMC solution of Ref. [12]. However, both DSMC solutions deviate from the approximate analytical NS solution. This is expectable and more deviation is predictable by increase of Knudsen number or plates' velocity. It is observed that all velocity profiles are in good agreement with slight deviation in analytical solution. However deviation of analytical temperature profile from DSMC solutions is noticeable. It is also observed in the figure that heat flux coefficients are in good agreement. Also shear stress coefficients with slight deviations are in good agreement. The larger scatter in our simulation compared with DSMC simulation of Ref. [12] is due to smaller sample size used here.

3.2. Effect of molecular diameter (d)

First, we performed simulations to investigate the effects of molecular diameter. We focus on velocity, temperature, heat flux and shear stress distributions. The Mach and Knudsen numbers are kept constant (Kn = 0.1, M_{wall} = 1.05). As shown in Fig. 3(a), variation of the molecular diameter has no effect on the bulk velocity of the domain. The formulation for the macroscopic velocity in x-direction in the DSMC method is as below [21]:

$$U = \frac{1}{N}\sum_{p=1}^{N_t}\sum_{q=1}^{N_p} c_{i,p} \tag{8}$$

$c_{i,p}$ is the molecular velocity component in the x-direction, N_p is the number of molecules in the sampled field cell at the pth sampling time step, and N is the total number of molecules sampled during the total time steps of N_t in the field cell. It is observed that the macroscopic velocity in the domain is a function of molecular velocity. In the shear driven Couette flow the only cause of the molecular velocity is the moving plates. Therefore we focus on the interaction between the molecules and moving plates here. To have a constant Knudsen number and different molecular diameters for different cases, the number of simulated molecules will be different in each case. This is because of dependency of the mean free path in the initial gas on diameter ($\lambda_0 = 1/\sqrt{2}\pi d^2 n$). In other words, in order to have the same degree of rarefaction, the number of molecules with smaller diameter would be higher. As a result, in a gas with smaller molecular diameter, the number of molecules colliding with the moving wall is higher and vice versa. However, the amount of absorbed macroscopic kinetic momentum is the same for both cases. The nonlinearity observed in velocity profiles near walls is due to the existence of *Knudsen layer*. The Knudsen layer is a kinetic boundary layer on the order of a mean free path (about one to a few mean free paths) and starts to become dominant between the bulk flow and solid surfaces in the transition flow regime [22]. For high Knudsen number flows (Kn > 1), this layer occupies whole the channel length. The velocity distribution and other physical variables are subject to appreciable changes within the Knudsen layer [23]. For example, as Gallis et al. [24] reported, within the Knudsen layer molecules collide with the surface more frequently than they collide with each other. For further discussions on Knudsen layer see Refs. [25–27].

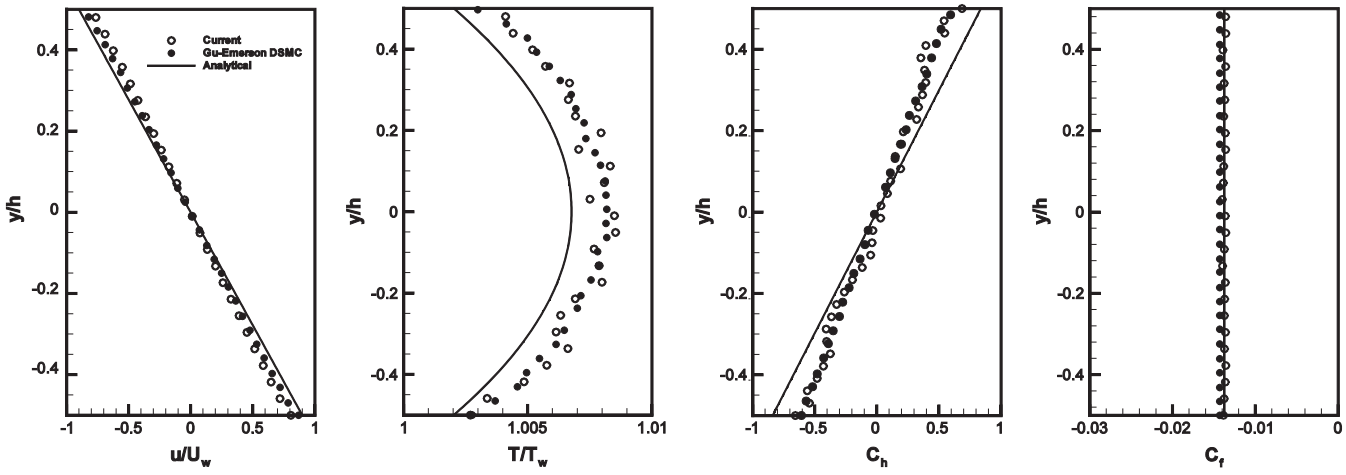

Fig. 2. Validation of results (Kn = 0.1, M_{wall} = 0.21).

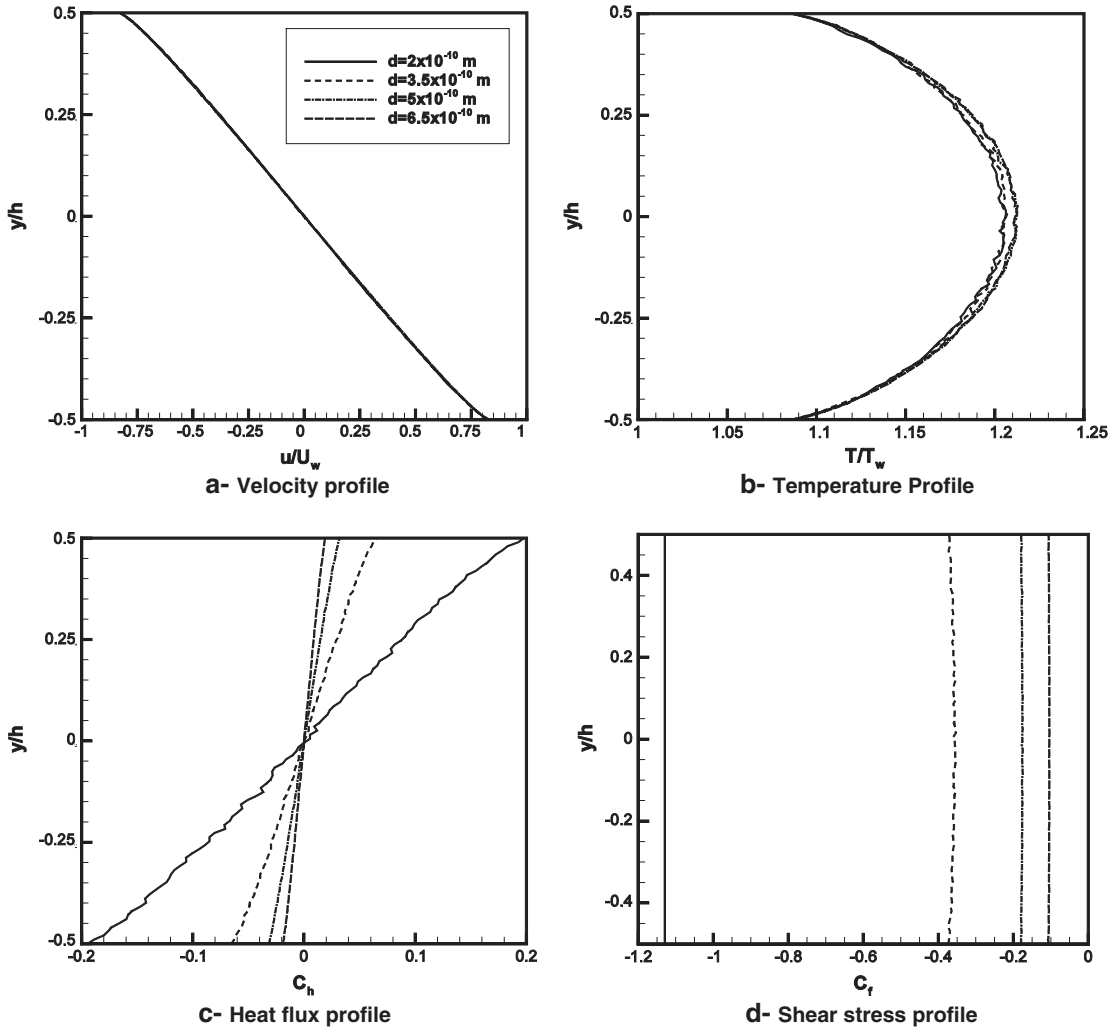

Fig. 3. Study of effects of molecular diameter on gas behavior.

The definition of temperature in molecular gas dynamics is given as follows:

$$T_x = \frac{m}{k}\left\{\frac{1}{N}\sum_{p=1}^{N_t}\sum_{q=1}^{N_p} {c_{i,p}}^2 - \left(\frac{1}{N}\sum_{p=1}^{N_t}\sum_{q=1}^{N_p} c_{i,p}\right)^2\right\} \tag{9}$$

$$T_y = \frac{m}{k}\left\{\frac{1}{N}\sum_{p=1}^{N_t}\sum_{q=1}^{N_p} {c_{j,p}}^2 - \left(\frac{1}{N}\sum_{p=1}^{N_t}\sum_{q=1}^{N_p} c_{j,p}\right)^2\right\} \tag{10}$$

$$T_z = \frac{m}{k}\left\{\frac{1}{N}\sum_{p=1}^{N_t}\sum_{q=1}^{N_p} {c_{k,p}}^2 - \left(\frac{1}{N}\sum_{p=1}^{N_t}\sum_{q=1}^{N_p} c_{k,p}\right)^2\right\} \tag{11}$$

$$T = \frac{1}{3}\left(T_x + T_y + T_z\right) \tag{12}$$

Similar to our previous discussion on the velocity profiles, we can justify the similar temperature profiles observed in Fig. 3(b). According to Eqs. (7)–(10), temperature is only a function of molecular velocity. However, as observed in Fig. 3(b), temperature profile in the center of the channel increases for molecules with larger diameter. This is due to increase of collision cross-section for molecules with larger diameters. Although in the case of molecules with larger diameter the number of molecules is less than what we simulate in case of molecules with small diameters, effect of collision cross-section increase is slightly more effective here. Therefore slight increase of temperature in the center of channel is observed by increasing the molecular diameter.

Fig. 3(c) and (d) show that non-dimensional heat flux and shear stress decrease as molecular diameter increases. According to Eqs. (1) and (3), it is observed that these two quantities are function of the density. The density, itself is a function of number of molecules and their mass. As we discussed before, the number of simulated molecules with smaller diameters is more than molecules with larger diameters. Therefore greater magnitudes of heat flux and shear stress are logical for smaller molecules. On the other hand, the number of intermolecular collisions would increase as the number of the molecules increases and the viscous dissipation due to the collisions causes larger amounts of heat flux and shear stress coefficients.

3.3. Effect of degrees of freedom (ζ)

The different behavior of hydrodynamics and thermal properties monatomic, diatomic and polyatomic gas molecular structures are shown in Fig. 4. Fig. 4(a) indicates that using gases with different degrees of freedom and keeping other molecular structures such as molecular mass, diameter, viscosity–temperature index and reference temperature constant, the bulk velocity of the domain remains constant for the range of simulations performed here. This is because

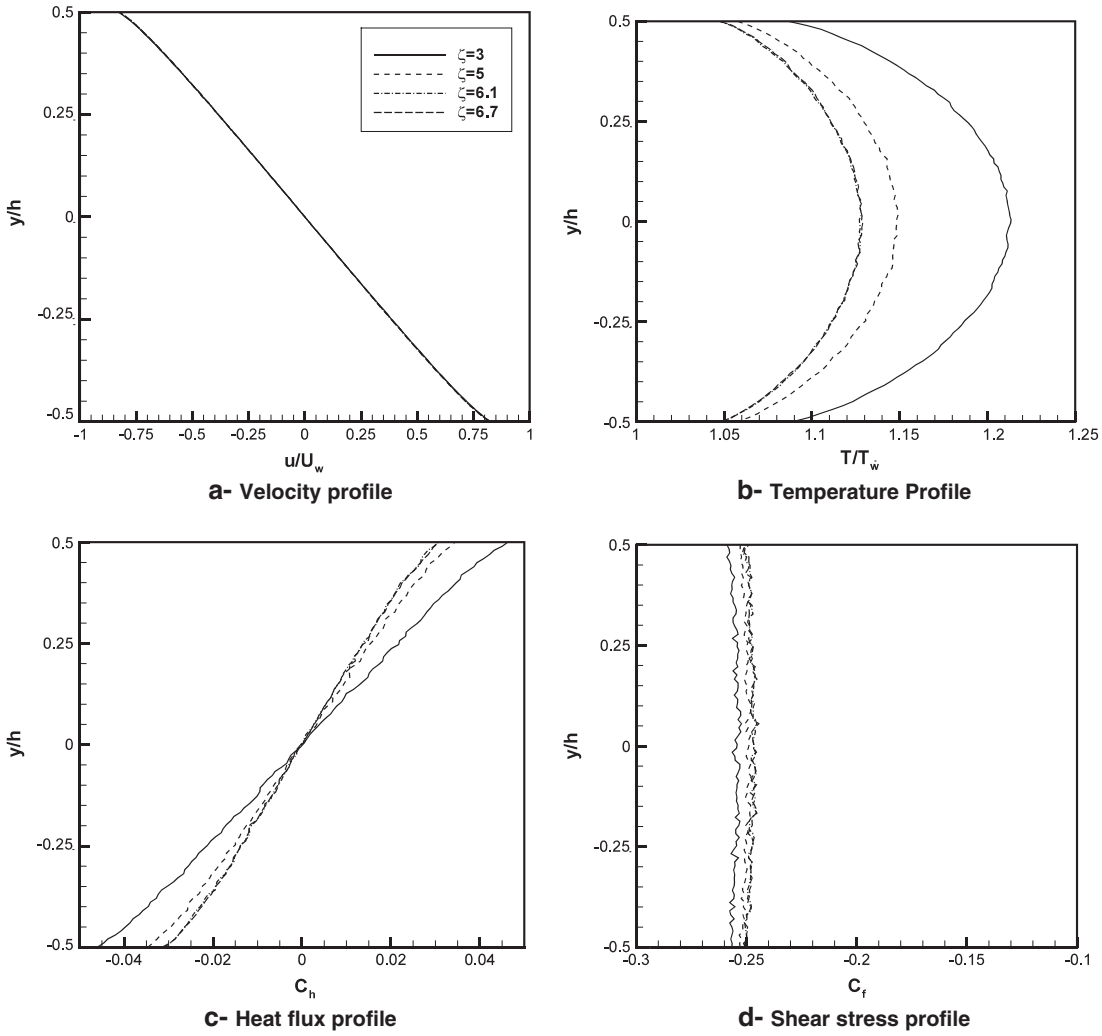

Fig. 4. Study of effects of degrees of freedom of molecules on gas behavior.

the macroscopic velocity only depends on the microscopic velocity of the molecules which is independent of the degree of freedoms of molecules. In other words, velocity profiles are shaped due to the momentum change after wall–molecules collisions. This change of momentum is not function of degree of freedom. However, other profiles show dependency of ζ. This is due to the variation of specific heat capacity (C_p) which is a function of the structure of gas. The relation between C_p and ζ is as follows:

$$C_p = \left(\frac{\zeta}{2} + 1\right)R \tag{13}$$

The energy of molecules may be stored in translational, rotational or vibrational modes. Monatomic molecules can only store energy in translational mode so that the degrees of freedom are just three in translational direction, but diatomic molecules may possess an additional three degrees of freedom for storing energy in rotational mode. In particular, the heat capacity depends on the number of degrees of freedom that are available to the particles in the gas to store thermal energy. The kinetic energy of gas particles is the only one of the many possible degrees of freedom which manifests as translational temperature change, and thus the larger the number of degrees of freedom available to the particles of a gas other than kinetic energy, the larger will be the specific heat capacity for the gas. Fig. 4(b) illustrates that temperature decreases once we simulate molecules with higher degrees of freedom. This decrease of temperature is explained by increase of the heat capacity due to using a gas with greater degrees of freedom instead of three. Fig. 4(c) also shows smaller amount of heat flux by increasing the degrees of freedom of molecules. This is also due to the increase of C_p. Simulating molecules with higher degrees of freedom shows that the energy is saved in molecules rather than transferring it as heat to the environment. The shear stress also experiences a decrease in absolute amount, which is shown in Fig. 4(d). As ζ increases, more momentum exchange in intermolecular collisions causes the shear stress in the domain decrease.

3.4. Effect of molecular mass (m)

Fig. 5(a) shows variation of velocity for gases with different molecular mass. It is observed that the velocity does not change considerably as the mass varies. The reason is that the molecular velocity is not related to the mass. It is observed in Fig. 5(b) that as the molecular mass increases the temperature also increases. This is obvious because the average kinetic energy for each molecule, mostly absorbed from the moving plates during the wall–molecule interactions, is proportional to the molecular mass [2].

$$e = \frac{1}{2}m\overline{c'^2} \tag{14}$$

It is also observed in Fig. 5(c) and (d) that the amount of non-dimensional heat flux and shear stress increases. These observations

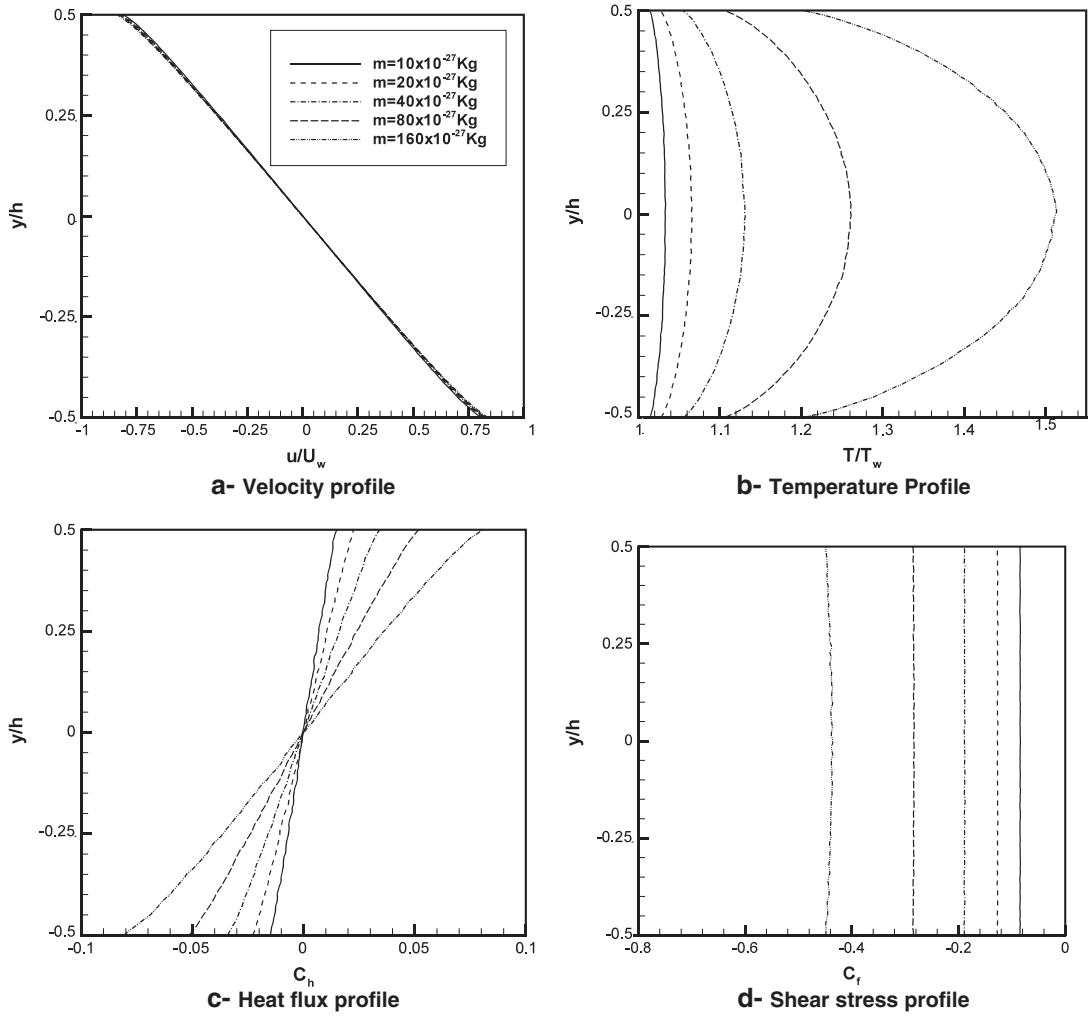

Fig. 5. Study of effects of molecular mass on gas behavior.

are quite consistent with the increase of the kinetic energy due to molecular mass increase. Since the shear stress is a function of transferred momentum from the plates which is dissipated, and the amount of total absorbed energy from the walls increases according to Eq. (14), this value increases as the molecular mass is increased.

3.5. Effect of viscosity–temperature index (ω)

The variation of velocity for three different viscosity–temperature indexes is shown in Fig. 6(a). One can see that the bulk velocity decreases when ω increases. This is because of increase of mean free path by increasing ω. The VHS relation between viscosity and the mean free path is defined according to [28]:

$$\lambda = (2\mu/15)(7-2\omega)(5-2\omega)(2\pi RT)^{-1/2}/\rho \tag{15}$$

Also the relation between viscosity and temperature according to the Chapman–Enskog expansion is defined as below [2]:

$$\mu = \mu_\infty (T/T_\infty)^{\omega} \tag{16}$$

Eqs. (15) and (16) show that increase of ω, increases μ and therefore λ. Increase of mean free path is equivalent to using a more rarefied gas. In this condition i.e., more rarefied flow, the number of the molecules colliding to the moving walls and transferring the kinetic momentum to the domain decreases. Therefore, the velocity in the domain decreases.

The increase of temperature shown in Fig. 6(b) is explained by increase of λ (or Knudsen number) due to increase of ω. As the flow becomes rarefied the constant energy absorbed from walls will be saved in smaller number of the molecules, and shows itself in terms of temperature rise. However in a less rarefied gas this amount of constant energy is distributed in larger number of molecules and the temperature rise is smaller than what is observed in more rarefied gases. Fig. 6(c) shows the variation of non-dimensional heat flux with viscosity–temperature index. The figure shows that the magnitude of heat flux increases for larger amounts of ω. This is because of increase of the surface–molecular collisions due to increase of the mean free path of the molecules. As a result, not only the molecules near the surface but also molecules in the center of channel can collide with the surfaces. Therefore, more absorbed kinetic energy from the wall is transferred into heat. Fig. 6(d) shows that the shear stress increases when we are facing with molecules which have larger amounts of ω. The reason is absorption of more momentum from the walls by increase of ω.

3.6. Multiple effects in real gases

At the final stage, simulations are performed for some real gases, i.e. hydrogen (H_2), nitrogen (N_2), argon (Ar), carbon dioxide (Co_2), chlorine (Cl_2), and xenon (Xe), to investigate the most effective

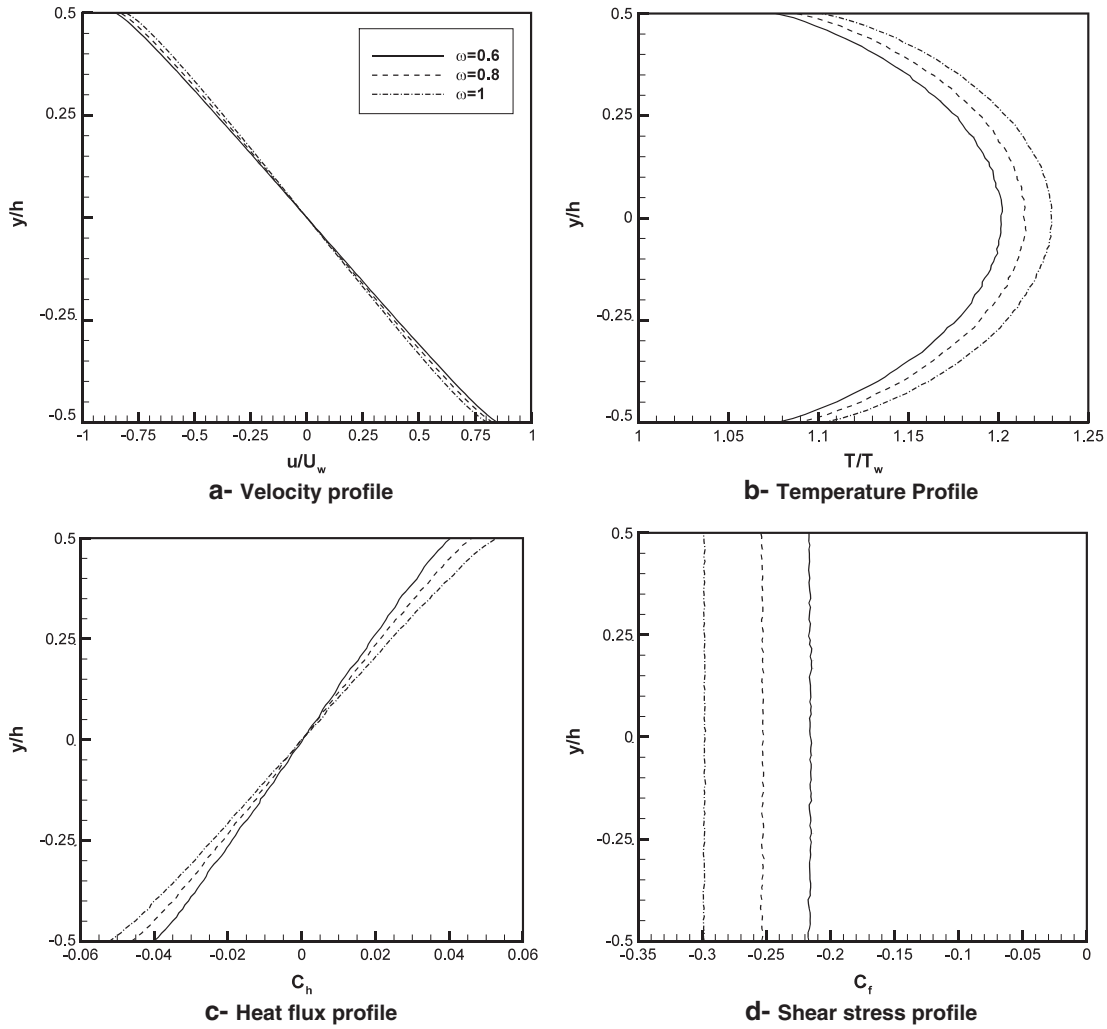

Fig. 6. Study of effects of degrees of viscosity–temperature index on gas behavior.

parameters on the velocity, temperature, heat flux and shear stress behavior of the gas. Simulated real gases are tabulated in Table 2. The reason for choosing these gases is to have a full coverage of all the molecular parameters. Fig. 7(a) shows the velocity profile for different gases. As it is observed in velocity profiles of Figs. 3–6, the effect of the viscosity–temperature index on the bulk velocity is the strongest effect among the four investigated parameters, which decreases the velocity in the domain as increases. Meanwhile it is observed that increase of mass has a reverse effect, i.e., slight increase of domain velocity. It is also observed in Table 2 that the molecular mass and viscosity–temperature index are in direct relation with each other. Simulation of real gases shows that for gases with molecular mass in the range of 46 to 118×10^{-10}, the increase of ω plays the key role. However for gases with sufficiently small or large masses like H_2 and Xe, the controlling parameter is m.

Table 2
Simulated cases: real gases (Kn = 0.1–M_{wall} = 1.05).

Gas	Diameter ($d\times10^{10}$ m)	Degrees of freedom (ζ)	Molecular mass ($m\times10^{27}$ kg)	Viscosity index (ω)
Hydrogen (H_2)	2.92	5	3.34	0.67
Nitrogen (N_2)	4.17	5	46.5	0.74
Argon (Ar)	4.17	3	66.3	0.81
Carbon dioxide (CO_2)	5.62	6.7	73.1	0.93
Chlorine (Cl_2)	6.98	6.1	117.7	1.01
Xenon (Xe)	5.74	3	218	0.85

Investigation of the effects of molecular parameters on temperature profiles in the previous sections shows that increasing m, d and ω results in temperature rise in the domain. It also seems that the molecular mass has the strongest effect on temperature. These three parameters are in direct relation with each other. However, increase of ζ decreases the temperature. Fig. 7(b) shows that the molecular mass and degrees of freedom are the competing parameters in temperature rise and fall. The figure shows that the increase of temperature is in direct relation with increasing the molecular mass. However, there is one exception, i.e., CO_2, a polyatomic gas with the degree of freedom of 6.7.

Fig. 7(c) is the non-dimensional heat flux profiles for real simulated gases. As discussed in the previous sections we know that increase of d and ζ decrease the absolute amount of C_h. On the other hand, increase of m and ω decreases this quantity. Looking at Table 2 and this figure, it is observed that the role of molecular mass and degree of freedom is more pronounced. It is observed that as the molecular mass increases the magnitude of heat flux increases but this trend is not valid for polyatomic molecules because their degree of freedom is larger than monatomic and diatomic gases.

In Fig. 7(d) the variation of shear stress coefficient is investigated. These variations are very similar to those observed for heat flux coefficient, i.e., increase of d and ζ decreases the absolute amount of C_f, but increase of m and ω decreases this quantity. In the same way we concluded in the last paragraph, we can see that molecular mass and degree of freedom are the major parameters and the expectable trend of

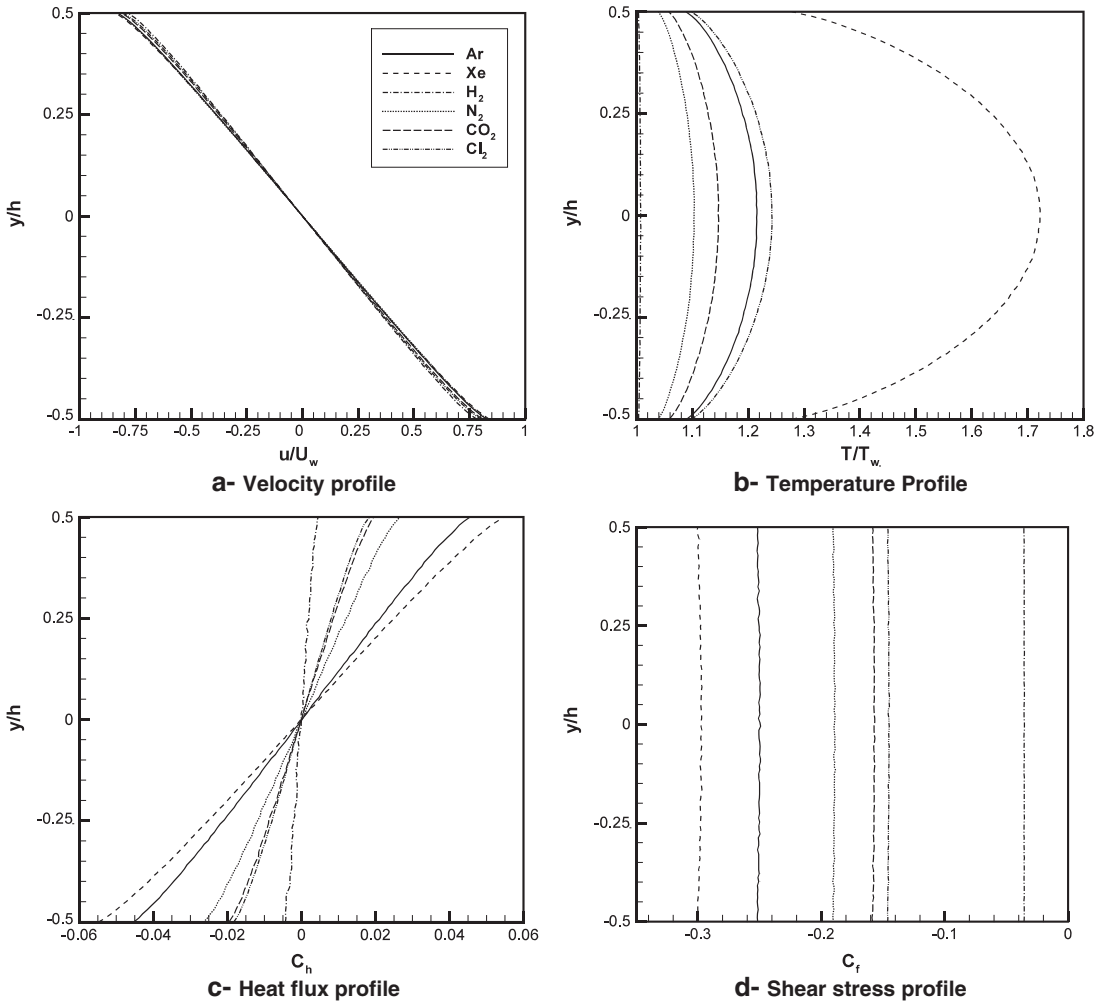

Fig. 7. Study of multiple effects of molecular structures on gas behavior.

increasing of C_f by increasing the molecular mass has two exceptions which are polyatomic gases.

4. Conclusion

In this paper, the classical problem of Couette flow was simulated for the investigation of the effects of four molecular gas structures, i.e., molecular diameter, mass, degree of freedom and viscosity–temperature index on hydrodynamics and thermal behaviors of rarefied flow using the DSMC method. The effects of variation of each of these parameters on the velocity, temperature, heat flux and shear stress coefficients were investigated in details for imaginary gases and the observed physics was justified. Then simulations were performed for real gases to see the multiple effects of these parameters and also to find the parameters which have the key role. The results show that increase of d, ζ, m has almost no effect on the bulk velocity of the domain in the simulated range. However increase of ω by 0.2 unit leads to increase of domain velocity near the walls about 2–3% of plates' velocity. It is observed that increase of d, m, and ω increases the temperature in the domain. This effect for molecular diameter is very slight. However increase of ζ decreases the temperature in the domain. It is also observed that increase of d and ζ decreases both heat flux and shear stress and increase of m and ω increases these quantities. Simulation of real gases shows that the main effective parameter on the bulk velocity is the viscosity–temperature index of the gas. In other profiles, i.e., temperature, heat flux and shear stress coefficients, molecular mass and degree of freedom play the key roles.

References

[1] G. Karniadakis, A. Beskok, N. Aluru, Micro Flows and Nano Flows: Fundamentals and Simulation, Springer-Verlag, New York, 2005.
[2] G.A. Bird, Molecular Gas Dynamics and the Direct Simulation of Gas Flows, Clarendon Press, Oxford, United Kingdom, 1994.
[3] D.L. Morris, L. Hannon, A.L. Garcia, Slip length in a dilute gas, Physical Review A 46 (8) (1992) 5279.
[4] A. Beskok, G.E. Karniadakis, W. Trimmer, Rarefaction and compressibility effects in gas microflows, Journal of Fluids Engineering 118 (3) (1996) 448–456.
[5] W. Marques Jr., G.M. Kremer, F.M. Sharipov, Couette flow with slip and jump boundary conditions, Continuum Mechanics and Thermodynamics 12 (6) (2000) 379–386.
[6] H. Xue, Q. Fan, C. Shu, Prediction of micro-channel flows using direct simulation Monte Carlo, Probabilistic Engineering Mechanics 15 (2) (2000) 213–219.
[7] H. Xue, H.M. Ji, C. Shu, Analysis of micro-Couette flow using the Burnett equations, International Journal of Heat and Mass Transfer 44 (21) (2001) 4139–4146.
[8] H. Xue, H. Ji, Prediction of flow and heat transfer characteristics in micro-Couette flow, Nanoscale and Microscale Thermophysical Engineering 7 (1) (2003) 51–68.
[9] M.J. McNenly, M.A. Gallis, I.D. Boyd, Empirical slip and viscosity model performance for microscale gas flow, International Journal for Numerical Methods in Fluids 49 (11) (2005) 1169–1191.
[10] S. Roy, S. Chakraborty, Near-wall effects in micro scale Couette flow and heat transfer in the Maxwell-slip regimes, Microfluidics and Nanofluidics 3 (4) (2007) 437–449.
[11] A. Frezzotti, L. Gibelli, B. Franzelli, A moment method for low speed microflows, Continuum Mechanics and Thermodynamics 21 (6) (2009) 495–509.
[12] X.J. Gu, D.R. Emerson, A high-order moment approach for capturing non-equilibrium phenomena in the transition regime, Journal of Fluid Mechanics 636 (2009) 177–216.

[13] Rakesh Kumar, E.V. Titov, D.A. Levin, Reconsideration of planar Couette flows using the statistical Bhatnagar–Gross–Krook approach, Thermopyhysics and Heat Transfer 24 (2010) 9.
[14] C. Cercignani, Rarefied Gas Dynamics. From Basic Concepts to Actual Calculations, Cambridge University Press, 2000.
[15] E. Roohi, M. Darbandi, Extending the Navier–Stokes solutions to transition regime in two-dimensional micro- and nanochannel flows using information preservation scheme, Physics of Fluids 21 (8) (2009) 082001.
[16] E. Roohi, M. Darbandi, V. Mirjalili, Direct simulation Monte Carlo solution of subsonic flow through micro/nanoscale channels, Journal of Heat Transfer 131 (9) (2009) 092402.
[17] M. Darbandi, E. Roohi, Study of subsonic–supersonic gas flow through micro/nanoscale nozzles using unstructured DSMC solver, Microfluidics and Nanofluidics 10 (2) (2011) 321–335.
[18] E. Roohi, M. Darbandi, Recommendations on performance of parallel DSMC algorithm in solving subsonic nanoflows, Applied Mathematical Modeling 36 (5) (2012) 2314–2321.
[19] M. Darbandi, E. Roohi, DSMC simulation of subsonic flow through nanochannels and micro/nano backward-facing steps, International Communications in Heat and Mass Transfer 38 (10) (2011) 1444–1449.
[20] J. Meng, Y. Zhang, Analytical solutions for the lattice Boltzmann model beyond Naviers–Stokes, Advances in Applied Mathematics Mechanics 2 (5) (2010) 670–676.
[21] W.W. Liou, Y. Fang, Microfluid Mechanics: Principles and Modeling, McGraw-Hill, 2006.
[22] Y. Sone, Kinetic Theory and Fluid Dynamics Birkhauser Boston, , 2002.
[23] C. Cercignani, Mathematical Methods in Kinetic Theory, Plenum Press, New York, 1990.
[24] M.A. Gallis, J.R. Torczynski, D.J. Rader, M. Tij, A. Santos, Normal solutions of the Boltzmann equation for highly nonequilibrium Fourier flow and Couette flow, Physics of Fluids 18 (1) (2006) 017104.
[25] X.J. Gu, D.R. Emerson, A computational strategy for the regularized 13 moment equations with enhanced wall-boundary conditions, Journal of Computational Physics 225 (1) (2007) 263–283.
[26] C. Lilley, J. Sader, Velocity gradient singularity and structure of the velocity profile in the Knudsen layer according to the Boltzmann equation, Physical Review E - Statistical, Nonlinear, and Soft Matter Physics 76 (2) (2007) 026315.
[27] S. Mizzi, R. Barber, D. Emerson, J. Reese, S. Stefanov, A phenomenological and extended continuum approach for modelling non-equilibrium flows, Continuum Mechanics and Thermodynamics 19 (5) (2007) 273–283.
[28] G.A. Bird, Definition of mean free path for real gases, Physics of Fluids 26 (11) (1983) 3222–3223.